Cytotoxicity Modulation of Ruthenium (II) tris-bathophenantholine Complexes With Systematically Varied Charge.

Hassib Audi,[a,‡] Daniel Azar,[a,‡] Farah Mahjoub,[a] Stephanie Farhat,[a] Zeinab El-Masri,[a] Mirvat El-Sibai,[a] Ralph J. Abi-Habib[a] and Rony S. Khnayzer[a,*].

[a] Department of Natural Sciences, Lebanese American University, Chouran, Beirut 1102-2801, Lebanon.

KEYWORDS ruthenium tris-bathophenanthroline, cancer, singlet oxygen, charge effect.

ABSTRACT: A series of four ruthenium (II) complexes $Ru(bp)_n(bps)_{3-n}$ (n = 0-3; bp = 4,7-diphenyl-1,10-phenanthroline or bathophenanthroline; and bps = disulfonated 4,7-diphenyl-1,10-phenanthroline or bathophenanthroline disulfonate) bearing different charges were synthesized and characterized. In aqueous media, all complexes displayed similar photophysical properties which makes this series ideal to study the effect of charge on the cytotoxicity of Ru(II) complexes. $Ru(bp)_3^{2+}$ (**1**) and $Ru(bps)_3^{4-}$ (**4**) are known photosensitizers that penetrate cancer cells and possess a significant light-induced cytotoxicity. The newly conceived neutral $Ru(bp)_2(bps)^0$ (**2**) and dianionic $Ru(bp)(bps)_2^{2-}$ (**3**) were also found to have significant uptake as well as light-activation properties. Importantly, upon systematic modulation of complexes charge, the dark cytotoxicity was successfully tuned. The cationic complex **1** was potent against 5 out of 6 cell lines tested (MDA-MB-231, MCF-7, B16, SF and ML2) and displayed the highest cytotoxicity with IC_{50} values of 4.0, 3.6, 1.7, 1.0 and 2.9 μM, respectively. The two anionic complexes, **3** and **4**, with overall charges of -2 and -4, were not potent against any of the cell lines in the dark (IC_{50} > 200 μM), whereas the neutral molecule, complex **2**, was potent against 3 out of 6 cell lines in the dark (B16, SF and ML2) and exhibited an intermediate activity with IC_{50} values of 12.8, 3.0 and 10.3 μM, respectively. All complexes presented significant phototoxicity when activated at 6 h post-incubation, which is consistent with their fast uptake and ability to produce singlet oxygen. Localization of complexes **1-4** within the cells were found to be dependent on the charge and photoexcitation conditions. The charge-activity relationship elucidated in this work facilitates the development of new sensitizers for photodynamic therapy.

1. INTRODUCTION

Cancer is a disease typically detected at a late stage leading to high mortality rates among patients.[1-2] It is often correlated with the formation of tumors due to uncontrolled malignant cell growth in undesired areas of the body.[3] To date, there is a lack of cancer-curing drugs that are efficient, specific and possess little to no side effects. Cisplatin and its analogues are common chemotherapeutic agents used to treat cancer patients.[2, 4-5] These Pt(II) transition metal complexes are highly potent and are commonly associated with severe side effects and/or drug resistance which compromise their effectiveness in therapy.[6] The mechanism of action of cisplatin was extensively investigated and summarized in detailed review articles.[7-8] It was found that the active species leading to cross-reactivity of cisplatin with DNA is the Pt(II)-aqua complexes that results from chloride substitution by water.[9-10] In order for the drug to have minimal side effects, the most intuitive strategy is to specifically target cancer cells through a distinct mechanism, which is often expensive and exclusive to the type of cancer targeted. Photodynamic therapy (PDT), a process that utilizes light to drive therapeutic processes, is known for several decades and is clinically applied to treat certain types of diseases such as psoriasis, vitiligo and skin cancer.[11-13] The commonly investigated mechanisms of PDT focus on formation of singlet oxygen ($^1O_2$) and subsequently reactive oxygen species (ROS) as well as photobinding and cleavage of DNA.[12] In addition, the photochemical transformation of prodrugs to active potent molecules has been shown to be another effective mechanism that is worth investigating.[14] Based on these proposed mechanisms, several transition-metal complexes bearing varied ligand frameworks were designed and tested for their potency against human cancer cell lines.[14-24] Octahedral Ru(II) polypyridyl complexes are typically luminescent which facilitates the visualization of tumors through fluorescence imaging.[12] In addition, their absorption can be readily tuned through ligand modification to match the therapeutic window.[25-26] Importantly, Ru(II) octahedral complexes are active even in the presence of large quantity of glutathione, a molecule known to deactivate square planar Pt(II) complexes such as cisplatin.[7, 14, 27] The utilization of Ru(II) for photodynamic therapy of cancer was recently reviewed by Gasser and coworkers.[26] Different mechanisms of cancer cells death are plausible depending on the physical and chemical properties of the therapeutic agent. The production of reactive oxygen species (ROS) via quenching of triplet metal-to-ligand charge transfer (^{3*}MLCT) excited state is of prime importance in PDT.[28-31] A large amount of phenanthroline-based ligands[32] and ruthenium complexes[25-26, 33-36] coordinated to nitrogen and carbon based ligands were tested for their ability to kill cancer cells. Our research effort was focused on the synthesis and characterization of series of Ru(II) complexes bearing varied ligand frameworks. In previous studies, the dicationic Ru(II) tris-(bathophenanthroline) [$Ru(bp)_3^{2+}$ (**1**)] was found to intercalate with DNA[37-39] and was significantly toxic towards cancer cell lines[30]. However, the sulfonated tetraanionic counter-part, Ru(II) tris-(bathophenantholine disulfonate) [$Ru(bps)_3^{4-}$ (**4**)], was found to bind to proteins[40-41] and lacked any cytotoxicity in the dark[30]. Interestingly, even anionic Ru(II) and Pt(II) complexes bearing bps ligands possessed significant cellular uptake.[30, 42] Here, we sought the synthesis and characterization of two new complexes, $Ru(bp)_2(bps)^0$ (**2**) and $Ru(bp)(bps)_2^{2-}$ (**3**), that together with **1** and **4** elucidate the effect of charge on the different chemical, physical and biological properties of these complexes.

2. EXPERIMENTAL SECTION

2.1 Instrumentation. Absorption data were acquired on a Shimadzu UV-1650PC spectrophotometer. Photoluminescence were measured on a FL/FS920 spectrofluorimeter from Edinburgh Instruments equipped with a 450 W Xe arc lamp and a Peltier cooled, red sensitive PMT (R2658P, Hamamatsu). Lifetimes and transient absorption data were collected on an LP920 laser flash photolysis system from Edinburgh Instruments. The excitation pump source was a Vibrant LD 355 II Nd:YAG/OPO system (OPOTEK), kinetic traces were collected with a PMT (R928 Hamamatsu) and transient absorption difference spectra using an iStar ICCD camera (Andor Technology). Origin 8.1 was used for fitting kinetic traces. Real-time absorbance was measured using an ocean optic spectrometer (HR2000+) coupled to a deuterium/halogen light sources (DT-MINI-2-GS, Ocean Optics). Transmittance was acquired at a right angle of an incident He/Cd laser excitation (λ_{exc} = 442 nm and $P_{incident}$ = 30 mW). ^{1}H spectra were recorded on an AC500 Bruker spectrometer operating at 500 MHz. Chemical shifts are reported in delta (δ) units, expressed in parts per million (ppm) using the residual protonated solvent as an internal standard DMSO-d_6 2.50 ppm. The multiplicity of signals is designated by the following abbreviations: s, singlet; d, doublet; dd, doublet of doublets; m, multiplet. HPLC data were acquired on a Shimadzu quaternary pump coupled with a PDA detector and equipped with C18 column (Column Technologies Inc.) and fitted with a Phenomenex guard column using a published method.[14] High-resolution ESI-MS measurements were performed at MSU Mass Spectrometry Core Facility; MALDI-TOF MS at LAU proteomics facility (4800 PLUS MALDI TOF/TOF Analyzer from AB Sciex); and elemental analyses at Atlantic Microlab facilities, USA.

2.2 Materials. LiCl, $RuCl_3.3H_2O$, bathophenanthrolinedisulfonic acid disodium salt trihydrate (Na_2bps.$3H_2O$), bathophenanthroline (bp), tetrabutyl ammonium chloride (TBACl), 4′,6-Diamidino-2-phenylindole dihydrochloride (DAPI nucleic acid stain), and all solvents were obtained from Aldrich and used without any further purification.

2.3 Syntheses.

2.3.1 $Ru(bps)_2Cl_2$ and $Ru(bp)_2Cl_2$ were prepared in near quantitative yields by literature methods.[43-44] According to NMR studies,[45] the predominate isomer for sulfonate is the meta substituted as depicted by Figure 1.

2.3.1 $Ru(bp)_3Cl_2$ (1): This complex was prepared by modified literature methods.[44, 46] $RuCl_3.3H_2O$ (0.191 mmol) and bp (0.75 mmol) were added to 10 ml of N_2 degassed ethylene glycol. The mixture was refluxed for 4 h under nitrogen. After cooling to room temperature, a saturated aq. KPF_6 solution was added produced a dark orange precipitate that was collected by vacuum filtration. The product was dissolved in the minimum amount of acetone and saturated aq. TBACl solution was then added to produce an orange precipitate that was collected by vacuum filtration and purified by column chromatography (Sephadex column; eluent: EtOH). The orange band was collected and evaporated to afford the desired product as orange solid (yield 67%). ^{1}H NMR (dmso-d_6, 500 MHz): δ 8.37 (d, J=5.5 Hz, 6H), 8.29 (s, 6H), 8.85 (d, J=5.5 Hz, 6H), 7.72-7.61 (m, 30H). MALDI-TOF MS (m/z, amu): 1098.08 $[M]^+$.

2.3.2 $Ru(dp)_2(bps)$ (2): $Ru(bp)_2Cl_2$ (0.090 mmol) and bps ligand (0.099 mmol) were added to 10 mL of N_2-degassed 1:1 ethanol/water mixture. The mixture was heated at 90°C for 4h under nitrogen. The solvents were removed by rotavapor and the residue was dissolved in 2 mL of methanol and added dropwise to 300 mL of rapidly stirred diethyl ether. The orange precipitate was filtered, washed with diethyl ether, and dried under reduced pressure. The crude product was dissolved in the minimum amount of methanol and purified by column chromatography (LH-20 Sephadex column; eluent: methanol). The orange band was collected and evaporated to afford the desired product as orange solid (yield 67%). ^{1}H NMR (dmso-d_6, 500 MHz): δ 8.52-8.50 (m, 6H), 8.42 (s, 4H), 8.37 (s, 2H), 8.03 (s, 2H), 7.919-7.98 (m, 4H), 7.95-7.93 (m, 4H), 7.84-7.75 (m, 24H). MALDI-TOF MS (m/z, amu): 1257.12 $[M+H]^+$.

2.3.3 $Ru(bps)_2(bp)Na_2$ (3): $Ru(bps)_2Cl_2$ (0.071 mmol) and bp ligand (0.096 mmol) were added to 10 mL 1 of N_2-degassed 1:1 ethanol/water mixture. The mixture was heated at 90°C for 4h under nitrogen. The solvents were removed by rotavapor and the residue was dissolved in 2 mL of methanol and added dropwise to 300 mL of rapidly stirred diethyl ether. The orange precipitate was filtered, washed with diethyl ether, and dried under reduced pressure. The crude product was dissolved in the minimum amount of methanol and purified by column chromatography (LH-20 Sephadex column; eluent: methanol). The orange band was collected and evaporated to afford the desired product as orange solid (yield 82%). ^{1}H NMR (dmso-d_6, 500 MHz): δ 8.42 (d, J=5.5 Hz, 2H), 8.36 (t, 4H), 8.26 (s, 2H), 8.26-8.19 (m, 4H), 7.91 (d, J=9.5 Hz, 4H), 7.84 (d, J=12 Hz, 2H), 7.70-7.59 (m, 18H). EA calculated for $C_{72}H_{44}N_6Na_2O_{12}RuS_4.12H_2O$: C 51.58%; H 4.09%; N 5.01%, found: C 51.73%; H 3.95%; N 5.22%. ESI-TOF HRMS ($[M]^{2-}$) m/z calcd for $C72H44N6O12RuS4^{2-}$ 707.0480, found 707.0469.

2.3.4 $Ru(bps)_3Na_4$ (4): This complex was prepared by a literature method.[44] ^{1}H NMR (dmso-d_6, 500 MHz): δ 8.39 (d, J=5.5 Hz, 6H), 8.19 (s, 6H), 7.91 (s, 6H), 7.81-7.79 (m, 12H), 7.65-7.59 (m, 12H).

2.4 Proliferation Inhibition Assay (cytotoxicity). Cytotoxicity assays were carried out as described previously.[47-48] Cells were plated in flat-bottom 96-well plates at a density of 2-3 x10^4 cells/well in100 µL of their respective growth medium. Four-fold serial dilutions of the different complexes were made directly in the cell culture medium in round-bottom, 96-well plates to yield a total of 9 concentration points, in triplicates, ranging from 50 to 0.003 µM. Compound dilutions were then directly transferred to the cell plates containing the cells. The wells at all edges were left free of cells in order to prevent edge effect. An additional row with only the complexes was added as a control for their effect. DMSO corresponding to the volume of DMSO contained in the compound dilutions was also tested in duplicates. In the case of light activation, plates were exposed to blue LED light (LED Engin, 460 nm output, 130 lm at full-power, coupled with a focusing lens and a home-built LED dimmer) for 30 minutes either 6, 12 or 24 hrs after cell incubation with the complexes. Plates were then incubated for 72 hrs at 37 °C, 5% CO_2. Detection of cell viability was performed using the XTT Cell Proliferation Assay – Roche, as per manufacturer's instructions. Briefly, 50 uL of the XTT mixture was added to each well and the plates were incubated for 4 hrs at 37 °C. Absorbance was then read at 450 nm using a Varioscan Microplate Reader with linearity up to 4. All graphs were plotted and analyzed using GraphPad Prism 5 software.

2.5 Measurement of complex uptake. Cells ($3x10^5$ cells/well in 250 µL) were plated in 24-well plates overnight in their respective growth media. The required doses of the different complexes were diluted in cell culture medium as described above, and added to the plates in order to reach a total volume of 500 µL/well. The plates were incubated at 37°C with 5% CO_2 for 15 and 30 min, 1h, 2h and 6h, before being harvested and run for fluorescence detection on the FL3-H channel using BD Accuri C6 flow cytometer (BD Accuri, Ann Arbor, MI).

2.6 Cell cycle analysis. Cell cycle effect analysis was carried out using PI staining on flow cytometry as described previously.[49-50] Briefly, cells incubated with the different complexes (50 µM) or media alone for 6, 24 and 48 h at 37ºC/5% CO_2, were harvested and fixed in 70% ethanol for a minimum of 24 h, at -80ºC. Cells were then incubated with a PI staining solution (50 µg/ml) for 40 min at 37ºC. Samples were then read on a C6 flow cytometer (BD Accuri, Ann Arbor, MI) and total cell DNA content was measured on FL2-A with cells gated on width versus forward scatter.

2.7 Analysis of cell cytotoxicity. Type of cell death was determined using an Annexin V-fluorescin Isothiocyanate (Annexin V-FITC) and Propidium Iodide (PI) apoptosis detection kit (Abcam, Cambridge, MA) and a FITC-conjugated active caspase inhibitor (ApoStat Apoptosis Detection Kit, R&D Systems, Abingdon, England) on flow cytometry, as described previously.[49-50] Briefly, cells were incubated with either medium alone (control cells) or medium containing the different complexes at the highest concentration used in the cytotoxicity assay (50 µM) for 24 and 48 h at 37ºC/5% CO_2. Cells were then harvested and incubated with a FITC-conjugated annexin V antibody (2.5 mg/ml) and PI (5 mg/ml) for 45 min at 37ºC or incubated with 0.5 µg/ml of apostat for 30 min then harvested. Cells were then read using a C6 flow cytometer (BD Accuri, Ann Arbor, MI). Annexin V/PI data was analyzed on FL1-H versus FL2-H scatter plot and active caspases were detected on FL1-H. Cells were gated on width versus forward scatter.

2.8 Cell culture and immunostaining assay. Human mammary adenocarcinoma cells (MDA-MB-231) were cultured in DMEM medium supplemented with 10% FBS and 100 U penicillin/streptomycin at 37˚C and 5% CO_2. The cells were plated on cover slips 24 hours prior to the experiment. The cells were then treated independently with four different ruthenium(II) complexes for 6 hours. For the light activation, plates were exposed to blue LED light (as describe in section 2.4) after treatment with the complexes. Cells were then fixed with 4% para-formaldehyde for 10 min, and blocked with 1% BSA, in PBS for 1 hour. Samples were then stained with DAPI for 10 min. Fluorescent images were taken using a 60X objective on Axio observer Z1 fluorescent microscope (from Zeiss).

3. RESULTS

The design of new chemotherapeutic agents necessitates the understanding of structure-activity relationships. Given the large amount of variables in terms of functionalization of a ligand framework, we investigated the effect of overall Ru(II) complex charge on the photophysical, photochemical and biological activity of these complexes. To this end, we have successfully synthesized four octahedral complexes bearing a systematically varied number of bp and bps ligands. The complexes $Ru(bp)_3^{2+}$ (**1**); $Ru(bp)_2(bps)^0$ (**2**); $Ru(bp)(bps)_2^{2-}$ (**3**) and $Ru(bps)_3^{4-}$ (**4**) possess +2; 0; -2 and -4 overall charges respectively, Figure 1.

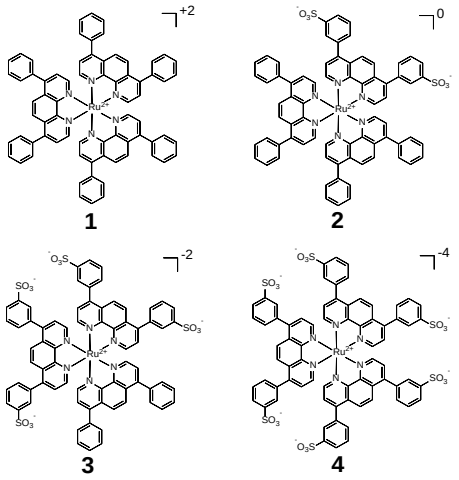

Figure 1. Chemical structures of a series of ruthenium complexes bearing different overall charges: $Ru(bp)_3^{2+}$ (**1**); $Ru(bp)_2(bps)^0$ (**2**); $Ru(bp)(bps)_2^{2-}$ (**3**) and $Ru(bps)_3^{4-}$ (**4**).

To glean insight into the electronic configuration of these ruthenium complexes, the normalized absorption and emission spectra of **1-4** were acquired in water at room temperature, Figure 2. It was found that the absorption and emission profiles are similar for all complexes irrespective of their charges, Figure 2. Photophysical assignments were done similar to known homoleptic Ru(II) complexes.[51] The lowest energy absorption band attributed to d → π^*_1 or MLCT was centered ~ 450 nm and composed of two shoulders, one ~ 433-437 nm and another ~ 461-464 nm. The broad and split nature of this band can be attributed to different vibronic contributors to this MLCT transition. The maximum extinction coefficients at that band for all four complexes were found ~ 29,300-30,000 $M^{-1}cm^{-1}$. Another MLCT band exist as a shoulder between 310-315 nm attributed to d → π^*_2 and a typical sharp π → π^*_1 was observed at 280 nm. The normalized absorption spectra in Figure 2 show that the neutral complex **2** is slightly different than the remaining 3 charged complexes which might be caused by partial aggregation or ion pairing in aqueous medium.[52-53] Typical structureless and broad triplet MLCT emission bands emanate from **1-4** with maximum intensity at ~ 620 nm giving rise to stokes shifts ~ 170 nm.

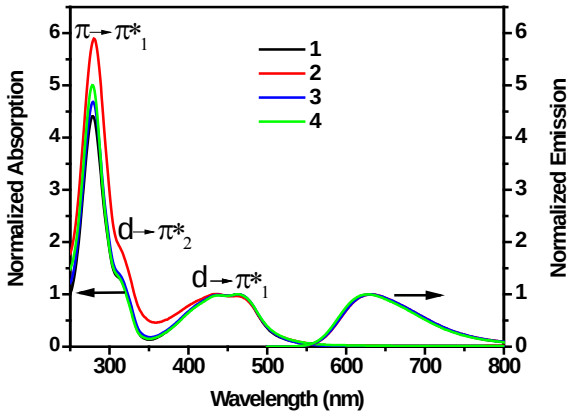

Figure 2. Normalized absorption and emission spectra (corrected for the detector's response) of complexes **1-4** in water.

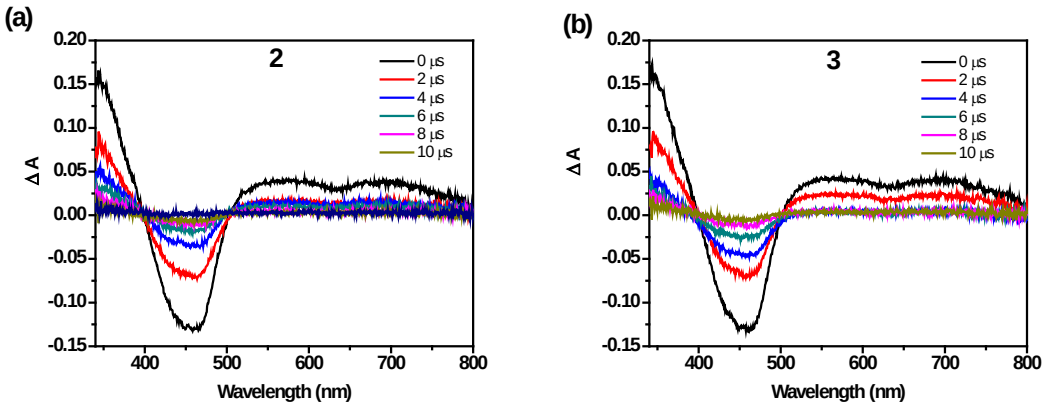

Figure 3. Transient absorption spectra of (**a**) **2** and (**b**) **3** in dearated water following 450 nm excitation with 2 µs sampling intervals. The triplet metal-to-ligand charge transfer excited state (^{3*}MLCT) shows broadband absorption features around 345, 575 and 700 nm whereas the ground state (GS) bleach is around 450 nm.

The nature of the emissive excited states of complexes **2** and **3** was investigated using nanosecond transient absorption (TA) spectroscopy. Samples in dearated water were pumped with 450 nm laser excitation (~ 5 mJ/pulse) and probed using white light. The difference absorption spectra were acquired at 2 µs delay intervals, Figure 3. The transients for complexes **2** (Figure 3a) and **3** (Figure 3b) show similar features: A ground state (GS) bleach centered around ~ 450 nm and excited state (ES) absorption at ~ 345 nm, 575 nm and 700 nm. For both complexes, single wavelength kinetics data acquired at 460 nm and 520 nm exhibited single exponential GS bleach recovery and ES decay with comparable lifetimes ~ 3.4-3.5 µs, Figure A1-A2.

Table 1 summarizes measured physical, photophysical, and photochemical properties of complexes **1**-**4**. The quantum yields of **1**-**4** increased from 0.051-0.061 to 0.200-0.248 upon degassing the aqueous solution, Table 1. This ~ 4 folds increase of quantum yield upon argon degassing of the aqueous solvent was paralleled with a similar increase in excited state lifetime from 0.75-0.87 µs to 3.38-3.67 µs, Figure A3-A4 and Table 1. The excited state lifetimes were acquired through photoluminescence decay data in aerated and dearated water solutions. All emission lifetimes fit single exponential decay functions and the values obtained for complexes **2** and **3** match the ones from TA spectroscopy, Figure A1-A4.

Table 1. Physical, photophysical and photochemical properties of complexes **1-4** in water.

Complex	1	2	3	4
Charge[a]	2	0	-2	-4
λ_{max} (nm)[b]	437, 462	433, 461	437, 462	437, 464
ε ($M^{-1}cm^{-1}$)	29,300[c]	30,000	27,300	29,500[c]
λ_{em} (nm)[d]	629	629	632	629
$\Phi_{PL,\ aerated}$[e]	0.055	0.051	0.055	0.061
$\Phi_{PL,\ deaerated}$[e]	0.23	0.2	0.21	0.248
$\tau_{aerated}$ (µs)[f]	0.75±0.04	0.86±0.07	0.87±0.07	0.86±0.04
$\tau_{deaerated}$ (µs)[f]	3.38±0.04	3.42±0.12	3.52±0.06	3.67±0.08
Φ_{Δ}[g]	0.47	0.46	0.47	0.48

[a] overall charge of the ruthenium complexes.

[b] maximum absorption wavelengths at the lowest energy MLCT absorption bands, see Figure 2.

[c] extinction coefficient from previous study.[46]

[d] maximum excited state emission wavelength following excitation at 450 nm, see Figure 2.

[e] relative quantum yield measured with $Ru(bpy)_3^{2+}$ [bpy = 2,2' bipyridine] in aerated water as standard with $\Phi_{PL} = 0.04$.[54]

[f] excited state lifetime following excitation at 450 nm.

[g] singlet oxygen quantum yield measured in D_2O versus TmPYP as standard with $\Phi_{\Delta} = 0.74$ at λ_{exc} = 436 nm.[55-56]

The substantial deactivation of the excited states of **1-4** by oxygen is crucial for efficient photochemical formation of ROS in aqueous solutions. The quenching of the ^{3*}MLCT by molecular oxygen is a traditional mechanism leading to the formation of $^1O_2$.[57-58] $^1O_2$ formation was probed in deuterated water since it possesses a long lifetime and detectable emission intensity in D_2O.[59] To gain insight into processes occurring in biological media upon photoexcitation, D_2O was chosen as a solvent. Using an infrared detector, the emission of $^1O_2$ was detected with peak at ~ 1275 nm[56] for complexes **1-4**, Figure 4. The quantum yield of $^1O_2$ formation (Φ_{Δ}) was found to be ~ 0.46-0.48 which is consistent with literature values in the case of **1** and **4**, Table 1.[30, 58] It is worth noting that the recorded $^1O_2$ emission spectra in all complexes suffered from a background noise. This noise is attributed to residual ^{3*}MLCT emission which was previously observed on the congener ruthenium(II) tris(2,2'-bipyridine) $Ru(bpy)_3^{2+}$ in D_2O using a similar setup to the one used in this study.[60] Time-resolved emission monitored at 1280 nm displayed a bi-exponential decay, with a short component attributed to the residual phosphorescence of $Ru(bpy)_3^{2+}$ and a longer component (59.47 µs) corresponding to $^1O_2$ lifetime in D_2O.[56] To further corroborate this hypothesis, **1** was measured in aerated D_2O and compared to the same solution degassed with Ar or O_2, Figure 4b. Increase in the background emission of **1** and disappearance of $^1O_2$ emission was observed in the deoxygenated solution purged with Ar, Figure 4b. However, as oxygen concentration increased in the solution, a significant decrease of background and a rise in the $^1O_2$ emission intensity was observed, Figure 4b.These results exemplified the quenching process of ^{3*}MLCT by dissolved O_2 yielding a decrease in the intrinsic emission from the complex and an increase in the $^1O_2$ emission in aerated solution.

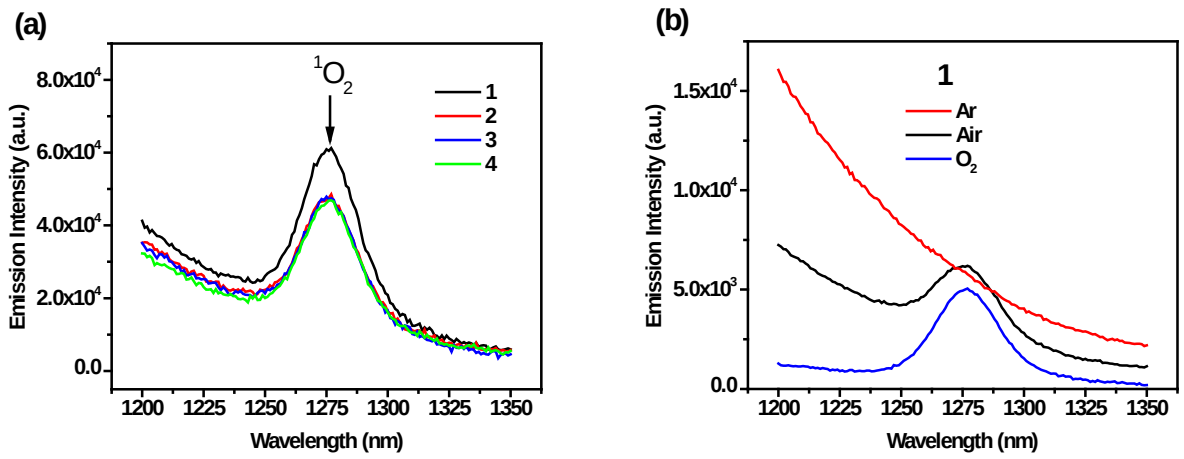

Figure 4. (a) Singlet oxygen ($^1O_2$) emission (indicated by an arrow) detected in the infrared region following photoexcitation (λ_{exc} = 450 ± 10 nm) of **1-4** in aerated D_2O. The emission was corrected for the detector's response. **(b)** Emission scan of a D_2O solution containing complex **1** under Ar degassed (red), aerated (black) and O_2 saturated (blue) conditions.

Photochemical dissociation of a ligand from ruthenium polypyridyl complexes is a well understood mechanism that occurs even in stable frameworks such as the prototypical ruthenium tris-bipyridine ($Ru(bpy)_3^{2+}$).[61-63] Since some ligands[32] and ruthenium aqua[14, 18, 31] complexes are active towards cancer cell lines, we have investigated the robustness of our complexes under high-power laser irradiation. Absorption changes typically signals the photochemical transformation to a photoproduct.[64] Absorption spectra of an aerated aqueous solution of **1-4** were measured in real-time as a function of He/Cd laser excitation (λ_{exc} = 442 nm, P = 33 mW), Figure A5. The kinetic traces of the absorbance values at 450 nm were extracted as a function of time, Figure 5. Both the absorbance values and the profile didn't change over time which signals a significant photostability of the complexes even under large photon flux.

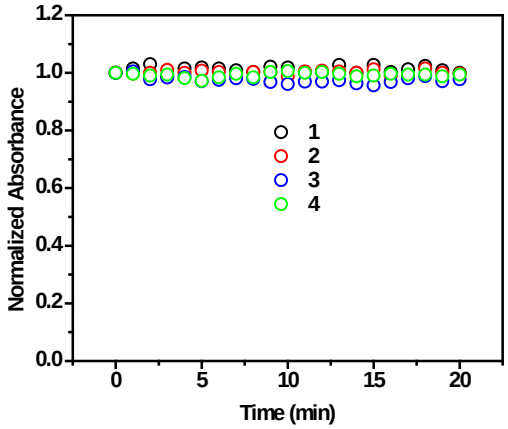

Figure 5. Normalized absorbance value at 450 nm of complexes **1-4** as a function of irradiation time in aerated water. The light source was He/Cd laser operated at 442 nm excitation and 33 mW incident power.

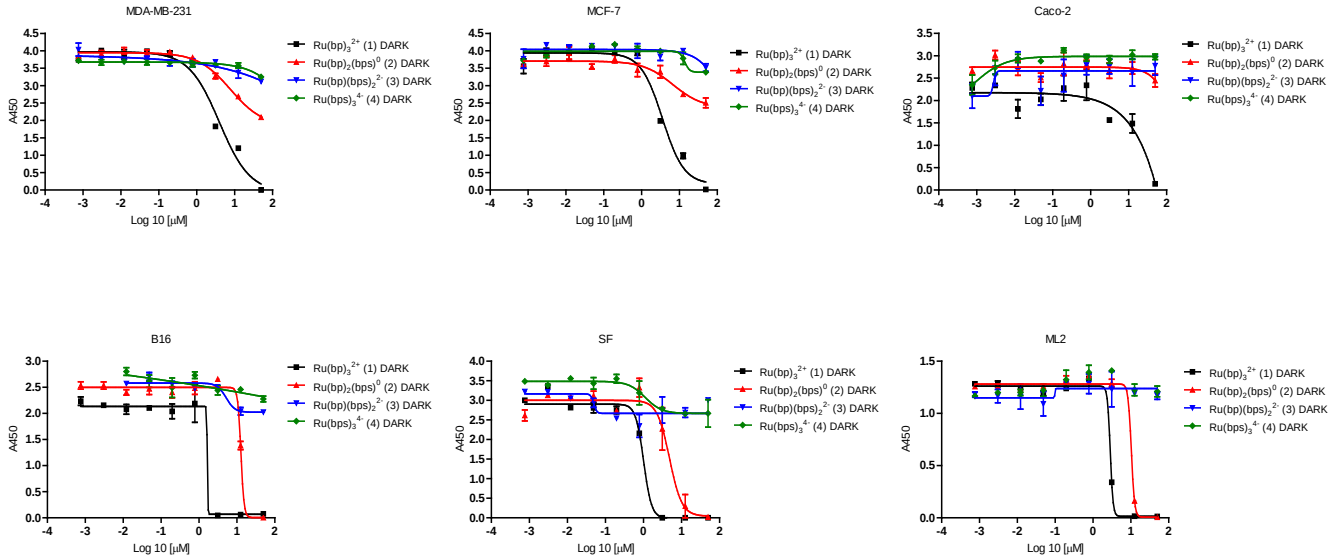

Figure 6. Cytotoxicity data of complexes **1** (black), **2** (red), **3** (blue) and **4** (green) on 6 different cell lines (MDA-MB 231, MCF-7, Caco-2, B16, SF and ML2). All complexes are measured in the dark after 72 hrs of incubation.

Table 2. IC_{50} expressed in µmol/L of complexes **1-4** in the dark after 72 hrs of incubation on 6 different cell lines (MDA-MB 231, MCF-7, B16, SF and ML2 and Caco-2).

Complex	1	2	3	4
MDA-MB-231	4	> 200	> 200	> 200
MCF-7	3.6	> 200	> 200	> 200
B16	1.7	13	> 200	> 200
SF	1	3	> 200	> 200
ML2	2.9	10	> 200	> 200
Caco-2	> 200	> 200	> 200	> 200

To determine whether charge variation of Ruthenium (II) tris-bathophenantholine complexes had an impact on their cytotoxicity, we tested the potency of complexes **1-4** to both hematological malignancies (the AML cell line ML2) and solid tumors (the breast cancer cell lines MDA-MB-231 and MCF-7, the Glioblastoma cell lines SF, the colon cancer cell line Caco-2 and the melanoma cell lines B16), both in the dark and following light activation (ML2 and SF). Only complex **1**, possessing a +2 overall charge, was potent against the majority of cell lines in the dark (5 out of 6) with only Caco-2 being resistant (IC_{50} > 200 µM). Complex **1** was potent against MDA-MB-231, MCF-7, B16, SF and ML2 with IC_{50} values of 4.0, 3.6, 1.7, 1.0 and 2.9 µM, respectively. Complex **2**, possessing a 0 overall charge, was only potent against 3 out of 6 cell lines in the dark (B16, SF and ML2) with IC_{50} values of 13, 3.0 and 10 µM, respectively. The two remaining complexes,

3 and **4**, with overall charges of -2 and -4, were not potent against any of the cell lines in the dark (IC_{50} > 200 μM) (Figure 6, Table 1). This demonstrates the structure function relationship of these complexes since their potency correlates with their overall charge. The complex carrying an overall charge of +2 was the most potent, in the dark, with potency decreasing for the non-charged complex and being completely abolished for the negatively charges complexes. It is worth noting that the cisplatin control on ML2 cell line yielded an IC_{50} of 4.0 μM which is at the same order of magnitude than complex **1**.

Additionally, the impact of light activation was tested at different time points on the potency of all 4 complexes against two cell lines SF and ML2 (most sensitive to complexes **1** and **2** in the dark). Light activation led to an equal increase in potency of all 4 complexes when applied at 6 hours post incubation with the complexes. However, when light activation was applied at later time points (12 and 24 hours post-incubation with the complexes) the potency of the different complexes varied significantly, reflecting potentially different cytotoxicity mechanisms based on the charge of each complex (Figure 7, Table 2).

Only complex **1** (positively charged) showed the same potency when light activated at 6, 12 and 24 hours post-incubation, while complex **2** (neutral) showed a decrease in potency when light activation was applied at 12 and 24 hours post-incubation compared to activation at 6 hours post-incubation. Complexes **3** and **4** (negatively charged) had a significant decrease in potency when activated at 12 hours compared to 6 hours post-incubation and completely lost potency when light activated at 24 hours post incubation with the complexes. We then investigated the uptake of the 4 complexes by the two cell lines tested above (ML2 and SF) using flow cytometry, Figure A12. Both cell lines showed significant uptake of all complexes tested starting as early as 15 min post-incubation with no differences being evident when comparing the uptake of the different complexes. These results, therefore, demonstrate that the uptake of these complexes by SF and ML2 cells occurs early, precedes the onset of cell death and is similar for all four complexes.

Cell cycle analysis of cells treated with complexes **1** and **2** at 6, 24 and 48 hours demonstrated that, in addition to their cytotoxic effect on cells, these complexes induced cell cycle arrest in the surviving fraction of cells at all time points tested, Figure A13. This was illustrated by the increase in the percentage of cells in the G0/G1 phase of the cell cycle (M1 gate) and decrease in the percentage of cells in the G2/M and S phases of the cell cycle (M2 and M3 gates) in treated cells compared to controls. The above indicates that complexes **1** and **2** exert a dual effect on cells inducing both significant cytotoxicity and cell cycle arrest in surviving cells. On the other hand, analysis of cell death type was performed using annexinV/PI and caspase staining. Positive staining for annexinV/PI in both cell lines after treatment with complexes **1** and **2** for 48 hours can be associated with either necrotic cell death or late-stage apoptotic cell death, Figure A14. Additionally, positive caspase staining indicated that caspases are active in both cell lines followed by treatment with **1** and **2**. The strong signs of caspase activation, along with positive annexinV staining, suggest an apoptotic type of cell death induced by these complexes.

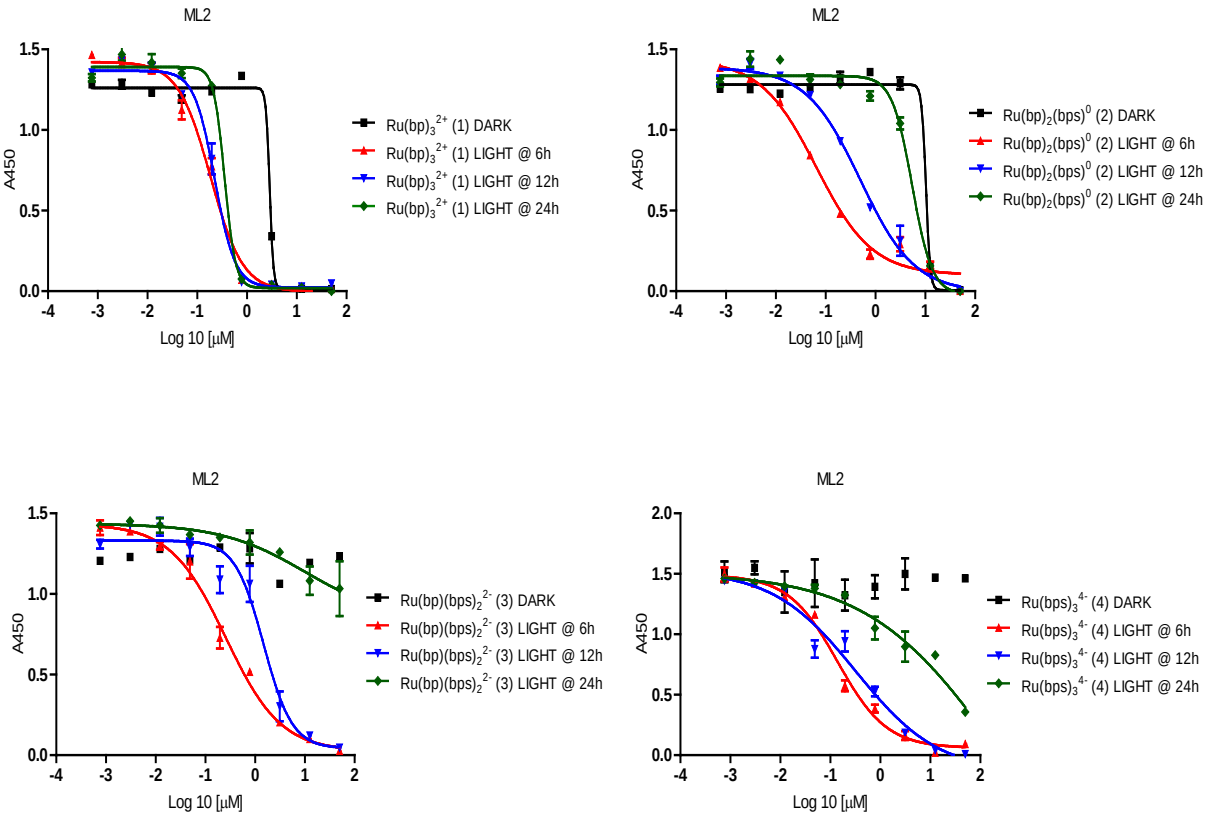

Figure 7. Cytotoxicity data of complexes **1-4** on ML2 cell lines in the dark (black) or photoactivated after 6h (red), 12h (blue) or 24 h (green). The reading was done after a total of 72 hrs incubation.

Table 3. IC_{50} expressed in µmol/L of complexes **1-4** on ML2 and SF cell lines following photoactivation after 6h, 12h or 24 h. The reading was done after a total of 72 hrs incubation.

Complex	**1**			**2**			**3**			**4**		
Activation time point	**6h**	**12h**	**24h**	**6h**	**12h**	**24h**	**6h**	**12h**	**24h**	**6h**	**12h**	**24h**
SF	0.1	0.1	0.2	0.8	2	12	0.4	0.2	>200	0.2	0.1	>200
ML2	0.2	0.2	0.3	0.1	0.5	5	0.3	1.5	>200	0.1	0.3	>200

Given the intrinsic photoluminescence of complexes **1-4** (Figure 2), fluorescence microscopy experiments were performed to glean insights on uptake and potential localization of these complexes in the nucleus versus the cytosol of MDA-MB231 cells, Figure 8. Cells were co-stained with DAPI, a known DNA staining agent. The cationic complexes **1** was clearly localized to the nucleus prior to light activation. However after light activation, complex **1** seemed to be excluded from the nucleus and cells looked apoptotic. The neutral complex **2** localized in a perinuclear fashion in the dark and likely became vesicular upon photoactivation. The dianionic complex **3** possessed poor uptake into cells in the dark as obviated by the small emission signal from within the cells versus the background. However, upon photoexcitation the uptake of **3** was elevated and this complex assumed a diffuse cytosolic pattern. The tetraanionic complex **4** was predominantly localized to the nucleus with slight diffuse cytosolic distribution in the dark. The latter stayed localized to the nucleus even after photoexcitation.

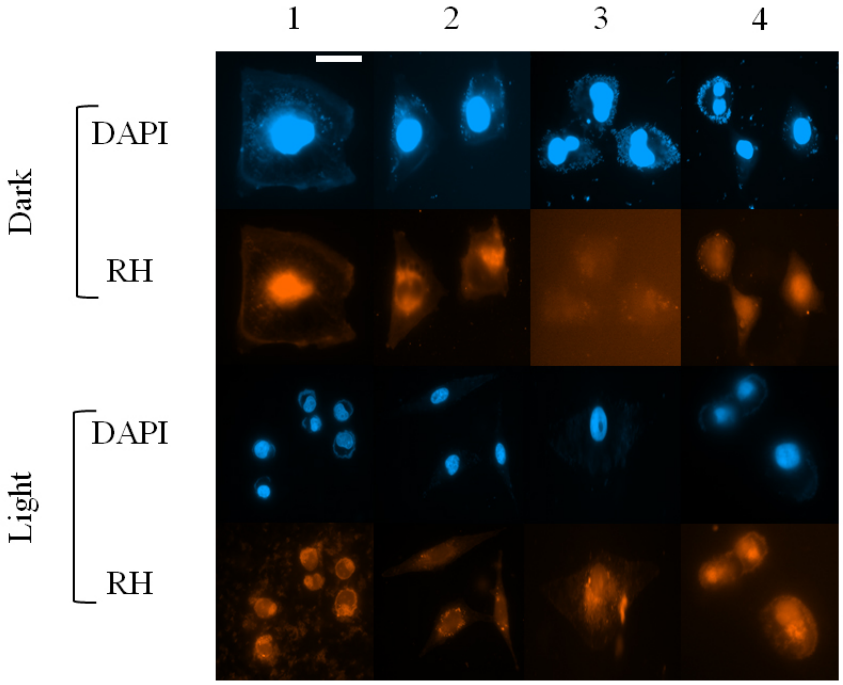

Figure 8. Localization of complexes **1-4** (Rhodamine filter/RH) in MDA-MB231 cells before and after light activation. Cells were treated independently with **1-4** for 6 hours. For the light activation (lower panel), plates were exposed to blue LED light after treatment with the complexes. Then the cells were fixed with 4% paraformaldehyde for 10 min, and blocked with 1% BSA, in PBS for 1 hour. Samples were stained with DAPI for 10 min before taking fluorescent images using a 60X objective on Axio observer Z1 fluorescent microscope (from Zeiss). Scale bar is 10 µm.

4. DISCUSSION

Ruthenium (II) polypyridyl complexes are gaining widespread popularity in the field of photodynamic therapy of cancer due to their rich and tunable photophysical and photochemical properties. Complexes **1-4,** possessing +2, 0, -2 and -4 overall charges respectively, were successfully synthesized and characterized. All these complexes were found to have similar photophysical properties irrespective of the degree of sulfonation and the overall charge. The significant quenching of excited state in aerated water and the large stokes shift indicate

that emission is phosphorescence emanating from a triplet metal-to-ligand charge transfer state (^{3*}MLCT), Scheme 1. The triplet nature of the excited state was further verified using transient absorption spectroscopy of complexes **2** and **3**. This ^{*3}MLCT is efficiently quenched by ground state $^3O_2$ to form $^1O_2$, Scheme 1. These results are consistent with typical ruthenium diimine complexes that exhibit near unity intersystem crossing efficiency.[65]

Importantly, it was found that the photophysical and photochemical properties of **1-4** are comparable, paving the way for studying the effect of charges on cytotoxicity with minimal change of other variables. The formation of $^1O_2$ following visible light absorption of **1-4** was detected owing to its infrared emission with peak around 1275 nm. **1-4** displayed the same quantum yield of singlet oxygen production within margin of error (Δ^1O_2 ~ 47 % in D_2O). Since all complexes yielded $^1O_2$, a well-known cell-damaging agent, light-activation of these complexes in cytotoxicity essays against cancer cell lines was deemed possible.

Scheme 1. Jablonski diagram of the photophysical and photochemical processes of complexes **1-4**. Following visible light absorption, (Abs.), molecules go from the ground state to the singlet metal-to-ligand charge transfer state (^{1*}MLCT) which undergo intersystem crossing (ISC) to yield triplet metal-to-ligand charge transfer state (^{3*}MLCT). The latter can return to the ground state via emission of light (Em.) termed phosphorescence or through non-radiative decay (dashed lines). Alternatively, the ^{3*}MLCT can be quenched by $^3O_2$ to form $^1O_2$ which is likely responsible of the photocytotoxicity of these complexes against cancer cell lines.

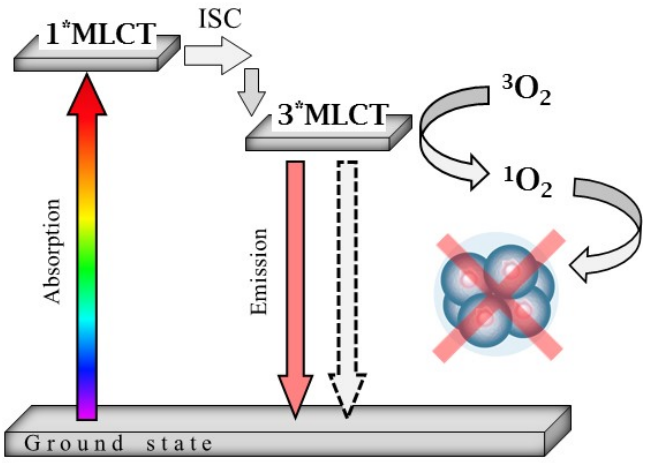

The photochemical stability of all complexes was investigated in the presence of high photon flux. This control was imperative to rule out any potential photochemical speciation of **1-4** in aqueous media.[66] Previous report have shown dual activity of complexes via the generation of $^1O_2$ and photochemical dissociation of caged transition metal complexes.[29, 67] However, we found that **1-4** are very stable for prolonged irradiation time with no sign of degradation or ligand loss over a period similar to the one utilized in photobiological experiments. These results strongly suggest that photosensitizers **1-4** operate by type II mechanism which leads to reactive oxygen species ($^1O_2$) that damage cancer cells by inducing oxidative stress.[12]

In the dark, the dicationic complex **1** was the most potent against an array of cell lines whereas the anionic complexes **3** and **4** were not cytotoxic at any concentration utilized with the neutral complex **2** possessing intermediate cytotoxicity. Our finding on this series are consistent with a previous report where complexes **1** and **4** were investigated.[30] In that study, complex **1** was found to localize to the mitochondria despite its high binding affinity to DNA, whereas complex **4** was localized to the cytosol.[30] All those findings support the argument that as the charge of the complex varies from +2 (complex **1**) to 0 (complex **2**) then -2 (complex **3**) and -4 (complex **4**), ability to bind negatively charged DNA and/or to localize to the mitochondria first decreases significantly leading to a decreased availability of the complex in the cell by 24 hours post-incubation. This led to a decrease in potency yielding a complete lack of activity for complexes **3** and **4** upon light activation at the late time points. The fast uptake of **1-4** into the cells observed in flow cytometry along with the photochemical formation of singlet oxygen was paralleled by the successful photoactivation of all complexes at early incubation time (6 h). However, the complete loss of light induced cytotoxicity of the anionic complexes at 24 h post-incubation indicate a possible efflux of **3** and **4** outside the cells as a function of time. Complex **2** also exhibits a gradual decline of photoactivation as the incubation time increases from 6 h to 24 h which might be also due to the efflux of this neutral complex outside the cell but at a slower rate than **3** and **4**. The cationic complex **1** didn't display significant time-dependent photoactivation which supports its binding or localization to organelles inside the cell. Cell cycle and cytotoxicity analyses performed on complexes **1** and **2** indicated dual effect on cells inducing both significant cytotoxicity likely through apoptotic pathways and cell cycle arrest in surviving cells. Fluorescence microscopy was then utilized to probe for nuclear localization of these complexes on MDA-MB231 cells incubated in the dark versus light. Complex **1** was found to co-localize with the nucleus in the dark and to be excluded from it upon photoexcitation. However, we can't rule out any specific localization to the mitochondria or lysosomes that was previously observed for complex **1** on A549 cells.[30] Complexes **2** and **3** displayed a perinuclear or cytosolic localization in the dark as well as upon photoexcitation. Albeit, the uptake of complex **3** notably improved when exposed to light. Complex **4** possessed nuclear localization with slight diffuse cytosolic localization in the dark and light. These results suggest that the overall charge of the complex can significantly change the localization of the complexes inside the cells as well as their biological targets and mode of action. In agreement with our results on this series of ruthenium complexes, Pavani et al. have previously shown a correlation between the increase in lipophilicity and zinc coordination of porphyrin ring with uptake and membrane interaction without altering the photophysical properties of the photosensitizers.[68-69] Importantly, exposure to light radically changed the localization of complex **1** which is consistent with results on TMPyP (5,10,15,20-tetrakis(N-methyl-4-pyridyl)-21H,23H-porphine) that demonstrated a relocalization from the nucleus to other microenvironment in cells upon light exposure.[70]

5. CONCLUSION

A series of Ru(II) complexes $Ru(bp)_n(bps)_{3-n}$ (where n=0-3) was investigated. A systematic change of charge was afforded by the variation of the degree of sulfonation in complexes **1-4**. The neutral (**2**) and dianionic (**3**) complexes are new molecules that were found to exhibit very similar photophysical and photochemical properties to their prototypical dicationic (**1**) and tetraanionic (**4**) counterparts. Upon photoexcitation of the complexes in aerated aqueous solutions, $^1O_2$ was formed via ^{3*}MLCT quenching and was verified by time-resolved and steady-state experiments. **1-4** were found to emit light from a triplet state (phosphorescence) with a quantum yield ~ 0.055 and lifetime ~ 0.8 μs in aerated water as well as Δ^1O_2 ~ 0.47 in aerated D_2O. In addition, after irradiation with light in aqueous solutions, no photochemical

dissociation of **1-4** was detected, demonstrating the robustness of these complexes even under high laser irradiance. The demonstrated photophysical and photochemical properties make complexes **1-4** attractive for fluorescence imaging and PDT. In-vitro cell culture assays using 6 different cell lines illustrated a correlation between the cytotoxicity of these complexes and their overall charge. In the dark, the positively charged complex (**1**) was the most potent with IC_{50} values ranging from 1 to 4 μM depending on the cell line. The negatively charged complexes, (**3** and **4**), had negligible cytotoxicity against all cell lines (IC_{50} > 200 μM). Finally, the neutral complex (**2**) had intermediate potency with IC_{50} values between 3 and 12.8 μM on three cell lines and IC_{50} > 200 μM on the remaining ones. All complexes showed enhancement of cytotoxicity when photoactivated at 6 h post-incubation which is consistent with their fast uptake and ability to produce singlet oxygen. However, the cytotoxicity of complexes **2-4** decreased when photoactivated at 24 h post-incubation indicating the possibility of efflux of these complexes out of the cells as a function of time. The positively charged complex **1** exhibited similar phototoxicity when activated at different time points, which is likely due to binding to biological targets or localization within organelles of the cells. Cell cycle and cytotoxicity analyses revealed apoptotic mechanism for cancer cell death in **1** and **2** whereas fluorescence microscopy experiments demonstrated a significant variation in the localization of complexes **1-4** in the nucleus and/or cytosol of cells as a function of complex charge and exposure to light. The structure-activity relationship established in this contribution can be of significance for the development of new molecular photosensitizer in the field of cancer therapeutics.

6. ACKNOWLEDGMENT

This work was funded by the School Research and Development Council at the Lebanese American University and the Lebanese National Council for Scientific Research (Ref: 05-06-14). We acknowledge Prof. Felix N. Castellano for useful discussions and for providing access to several instruments in his laboratory at NCSU. Karim El-Roz is thanked for assistance with singlet oxygen measurements.

7. REFERENCES

1. Ahmad, S., Platinum-DNA Interactions and Subsequent Cellular Processes Controlling Sensitivity to Anticancer Platinum Complexes. *Chem. Biodivers. 7* (3), 543-566.
2. Jamieson, E. R.; Lippard, S. J., Structure, recognition, and processing of cisplatin-DNA adducts. *Chem. Rev.* **1999,** *99* (9), 2467-2498.
3. Pinto, A. L.; Lippard, S. J., Binding of the antituour drug *cis*-diamminedichloroplatinum(II) (*cisplatin*) to DNA. *Biochem. Biophys. Acta* **1985,** *780*, 167-180.
4. Rosenberg, B.; Van Camp, L.; Krigas, T., Inhibition of Cell Division in Escherichia coli by Electrolysis Products from a Platinum Electrode. *Nature* **1965,** *205* (4972), 698-699.
5. Pil, P. L., S. J. In Encyclopedia of Cancer; Bertino, J. R., Ed.; *Academic Press*: San Diego, CA, 1997; Vol. 1.
6. Boulikas, T.; Vougiouka, M., Recent clinical trials using cisplatin, carboplatin and their combination chemotherapy drugs. *Oncol. Rep.* **2004,** (11), 559-595.
7. Fuertes, M. A.; Alonso, C.; Perez, J. M., Biochemical Modulation of Cisplatin Mechanisms of Action: Enhancement of Antitumor Activity and Circumvention of Drug Resistance. *Chem. Rev.* **2003,** *103* (3), 645-662.
8. Jung, Y. W.; Lippard, S. J., Direct cellular responses to platinum-induced DNA damage. *Chem. Rev.* **2007,** *107* (5), 1387-1407.
9. Miller, S. E.; House, D. A., The Hydrolysis Products of cis-Diamminedichloroplatinum(II). I. The Kinetics of Formation and Anation of the cis-Diammine(aqua)chloroplatinum(II) Cation in Acidic Aqueous Solution. *Inorg. Chem. Acta* **1989,** *161*, 131.
10. Lim, M. C.; Bruce Martin, R., The nature of cis amine Pd(II) and antitumor cis amine Pt(II) complexes in aqueous solutions. *J. Inorg. Nucl. Chem.* **1976,** *38* (10), 1911-1914.
11. Ackroyd, R.; Kelty, C.; Brown, N.; Reed, M., The History of Photodetection and Photodynamic Therapy. *Photochem. Photobiol.* **2001,** *74* (5), 656-669.
12. Dolmans, D. E. J. G. J.; Fukumura, D.; Jain, R. K., TIMELINE: Photodynamic therapy for cancer. *Nat. Rev. Cancer* **2003,** *3* (5), 380.

13. Vrouenraets, M. B.; Visser, G. W.; Snow, G. B.; van Dongen, G. A., Basic principles, applications in oncology and improved selectivity of photodynamic therapy. *Anticancer Res.* **2003,** (23), 505-522.
14. Howerton, B. S.; Heidary, D. K.; Glazer, E. C., Strained Ruthenium Complexes Are Potent Light-Activated Anticancer Agents. *J. Am. Chem. Soc.* **2012,** *134* (20), 8324-8327.
15. Mahnken, R. E.; Billadeau, M. A.; Nikonowicz, E. P.; Morrison, H., Development of photo cis-platinum reagents. Reaction of cis-dichlorobis(1,10-phenanthroline)rhodium(III) with calf thymus DNA, nucleotides and nucleosides. *J. Am. Chem. Soc.* **1992,** *114* (24), 9253-9265.
16. Wang, J.; Higgins, S. L. H.; Winkel, B. S. J.; Brewer, K. J., A new Os,Rh bimetallic with O2 independent DNA cleavage and DNA photobinding with red therapeutic light excitation. *Chem. Commun.* **2011,** *47* (35), 9786-9788.
17. Higgins, S. L. H.; Tucker, A. J.; Winkel, B. S. J.; Brewer, K. J., Metal to ligand charge transfer induced DNA photobinding in a Ru(ii)-Pt(ii) supramolecule using red light in the therapeutic window: a new mechanism for DNA modification. *Chem. Commun.* **2012,** *48* (1), 67-69.
18. Singh, T. N.; Turro, C., Photoinitiated DNA Binding by cis-[Ru(bpy)2(NH3)2]2+. *Inorg. Chem.* **2004,** *43* (23), 7260-7262.
19. Lutterman, D. A.; Fu, P. K. L.; Turro, C., cis-[Rh2(μ-O2CCH3)2(CH3CN)6]2+ as a Photoactivated Cisplatin Analog. *J. Am. Chem. Soc.* **2005,** *128* (3), 738-739.
20. Farrer, N. J.; Woods, J. A.; Munk, V. P.; Mackay, F. S.; Sadler, P. J., Photocytotoxic trans-Diam(m)ine Platinum(IV) Diazido Complexes More Potent than Their cis Isomers. *Chem. Res. Toxicol.* **2010,** *23* (2), 413-421.
21. Farrer, N. J.; Woods, J. A.; Salassa, L.; Zhao, Y.; Robinson, K. S.; Clarkson, G.; Mackay, F. S.; Sadler, P. J., A Potent Trans-Diimine Platinum Anticancer Complex Photoactivated by Visible Light. *Angew. Chem. Int. Ed.* **2010,** *49* (47), 8905-8908.
22. Loganathan, D.; Morrison, H., Effect of Ring Methylation on the Photophysical, Photochemical and Photobiological Properties of cis-Dichlorobis(1,10-Phenanthroline)Rhodium(III)Chloride†. *Photochem. Photobiol.* **2006,** *82* (1), 237-247.
23. Monro, S.; Scott, J.; Chouai, A.; Lincoln, R.; Zong, R.; Thummel, R. P.; McFarland, S. A., Photobiological Activity of Ru(II) Dyads Based on (Pyren-1-yl)ethynyl Derivatives of 1,10-Phenanthroline. *Inorg. Chem.* **2010,** *49* (6), 2889-2900.
24. Lincoln, R.; Kohler, L.; Monro, S.; Yin, H.; Stephenson, M.; Zong, R.; Chouai, A.; Dorsey, C.; Hennigar, R.; Thummel, R. P.; McFarland, S. A., Exploitation of Long-Lived 3IL Excited States for Metal-Organic Photodynamic Therapy: Verification in a Metastatic Melanoma Model. *J. Am. Chem. Soc.* **2012,** *135* (45), 17161-17175.
25. Knoll, J. D.; Turro, C., Control and utilization of ruthenium and rhodium metal complex excited states for photoactivated cancer therapy. *Coord. Chem. Rev.* **2015,** *282–283*, 110-126.
26. Mari, C.; Pierroz, V.; Ferrari, S.; Gasser, G., Combination of Ru(ii) complexes and light: new frontiers in cancer therapy. *Chem. Sci.* **2015,** *6* (5), 2660-2686.
27. Cepeda, V.; Fuertes, M. A.; Castilla, J.; Alonso, C.; Quevedo, C.; Perez, J. M., Biochemical Mechanisms of Cisplatin Cytotoxicity. *Anti-cancer Agent Me.* **2007,** (1), 3-18.
28. DeRosa, M. C.; Crutchley, R. J., Photosensitized singlet oxygen and its applications. *Coord. Chem. Rev.* **2002,** *233–234*, 351-371.
29. Knoll, J. D.; Albani, B. A.; Turro, C., New Ru(II) Complexes for Dual Photoreactivity: Ligand Exchange and 1O2 Generation. *Acc. Chem. Res.* **2015,** *48* (8), 2280-2287.
30. Dickerson, M.; Sun, Y.; Howerton, B.; Glazer, E. C., Modifying Charge and Hydrophilicity of Simple Ru(II) Polypyridyl Complexes Radically Alters Biological Activities: Old Complexes, Surprising New Tricks. *Inorg. Chem.* **2014,** *53* (19), 10370-10377.
31. Garner, R. N.; Gallucci, J. C.; Dunbar, K. R.; Turro, C., [Ru(bpy)2(5-cyanouracil)2]2+ as a Potential Light-Activated Dual-Action Therapeutic Agent. *Inorg. Chem.* **2011,** *50* (19), 9213-9215.
32. McCann, M.; Santos, A. L. S.; da Silva, B. A.; Romanos, M. T. V.; Pyrrho, A. S.; Devereux, M.; Kavanagh, K.; Fichtner, I.; Kellett, A., In vitro and in vivo studies into the biological activities of 1,10-phenanthroline, 1,10-phenanthroline-5,6-dione and its copper(ii) and silver(i) complexes. *Toxicol Res.* **2012,** *1* (1), 47-54.
33. Camm, K. D.; El-Sokkary, A.; Gott, A. L.; Stockley, P. G.; Belyaeva, T.; McGowan, P. C., Synthesis, molecular structure and evaluation of new organometallic ruthenium anticancer agents. *Dalton Trans.* **2009,** (48), 10914-10925.
34. Zhang, J.-X.; Zhou, J.-W.; Chan, C.-F.; Lau, T. C.-K.; Kwong, D. W. J.; Tam, H.-L.; Mak, N.-K.; Wong, K.-L.; Wong, W.-K., Comparative Studies of the Cellular Uptake, Subcellular Localization, and Cytotoxic and Phototoxic Antitumor Properties of Ruthenium(II)–Porphyrin Conjugates with Different Linkers. *Bioconjugate Chem.* **2012,** *23* (8), 1623-1638.
35. Barragán, F.; López-Senín, P.; Salassa, L.; Betanzos-Lara, S.; Habtemariam, A.; Moreno, V.; Sadler, P. J.; Marchán, V., Photocontrolled DNA Binding of a Receptor-Targeted Organometallic Ruthenium(II) Complex. *J. Am. Chem. Soc.* **2011,** *133* (35), 14098-14108.
36. Garza-Ortiz, A.; Maheswari, P. U.; Lutz, M.; Siegler, M. A.; Reedijk, J., Tuning the cytotoxic properties of new ruthenium(III) and ruthenium(II) complexes with a modified bis(arylimino)pyridine Schiff base ligand using bidentate pyridine-based ligands. *J. Biol. Inorg. Chem.* **2014,** *19* (4), 675-689.
37. Friedman, A. E.; Kumar, C. V.; Turro, N. J.; Barton, J. K., Luminescence of ruthenium(II) polypyridyls: evidence for intercalative binding to Z-DNA. *Nucleic Acids Res.* **1991,** *19* (10), 2595-2602.
38. Barton, J. K.; Basile, L. A.; Danishefsky, A.; Alexandrescu, A., Chiral probes for the handedness of DNA helices: enantiomers of tris(4,7-diphenylphenanthroline)ruthenium(II). *Proc. Natl. Acad. Sci. USA* **1984,** *81* (7), 1961-5.
39. Goldstein, B. M.; Barton, J. K.; Berman, H. M., Crystal and molecular structure of a chiral-specific DNA-binding agent: tris(4,7-diphenyl-1,10-phenanthroline)ruthenium(II). *Inorg. Chem.* **1986,** *25* (6), 842-847.
40. Rabilloud, T.; Strub, J.-M.; Luche, S.; Dorsselaer, A. v.; Lunardi, J., A comparison between Sypro Ruby and ruthenium II tris (bathophenanthroline disulfonate) as fluorescent stains for protein detection in gels. *Proteomics* **2001,** *1* (5), 699-704.
41. Lamanda, A.; Zahn, A.; Röder, D.; Langen, H., Improved Ruthenium II tris (bathophenantroline disulfonate) staining and destaining protocol for a better signal-to-background ratio and improved baseline resolution. *Proteomics* **2004,** *4* (3), 599-608.

42. De Pascali, S. A.; Migoni, D.; Papadia, P.; Muscella, A.; Marsigliante, S.; Ciccarese, A.; Fanizzi, F. P., New water-soluble platinum(II) phenanthroline complexes tested as cisplatin analogues: First-time comparison of cytotoxic activity between analogous four- and five-coordinate species. *Dalton Trans.* **2006,** (42), 5077-87.
43. Hackett, J. W.; Turro, C., Luminescent Ru(phen)n(bps)3-n2n-4 Complexes (n = 0−3) as Probes of Electrostatic and Hydrophobic Interactions with Micellar Media. *Inorg. Chem.* **1998,** *37* (8), 2039-2046.
44. Della Ciana, L.; Zanarini, S.; Perciaccante, R.; Marzocchi, E.; Valenti, G., Neutral and Dianionic Ru(II) Bathophenanthrolinedisulfonate Complexes: A Route To Enhance Electrochemiluminescence Performance in Aqueous Media. *J. Phys. Chem. C* **2010,** *114* (8), 3653-3658.
45. McDermott, G. P.; Zammit, E. M.; Bowen, E. K.; Cooke, M. M.; Adcock, J. L.; Conlan, X. A.; Pfeffer, F. M.; Barnett, N. W.; Dyson, G. A.; Francis, P. S., Evaluation of tris(4,7-diphenyl-1,10-phenanthrolinedisulfonate)ruthenium(II) as a chemiluminescence reagent. *Anal. Chim. Acta* **2009,** *634* (2), 222-227.
46. García-Fresnadillo, D.; Orellana, G., Interaction of Sulfonated Ruthenium(II) Polypyridine Complexes with Surfactants Probed by Luminescence Spectroscopy. *Helv. Chim. Acta* **2001,** *84* (9), 2708-2730.
47. Khoury, O.; Ghazale, N.; Stone, E.; El-Sibai, M.; Frankel, A. E.; Abi-Habib, R. J., Human recombinant arginase I (Co)-PEG5000 [HuArgI (Co)-PEG5000]-induced arginine depletion is selectively cytotoxic to human glioblastoma cells. *J. Neurooncol.* **2015,** *122* (1), 75-85.
48. Tanios, R.; Bekdash, A.; Kassab, E.; Stone, E.; Georgiou, G.; Frankel, A. E.; Abi-Habib, R. J., Human recombinant arginase I(Co)-PEG5000 [HuArgI(Co)-PEG5000]-induced arginine depletion is selectively cytotoxic to human acute myeloid leukemia cells. *Leuk. Res.* **2013,** *37* (11), 1565-71.
49. Kassab, E.; Darwish, M.; Timsah, Z.; Liu, S.; Leppla, S. H.; Frankel, A. E.; Abi-Habib, R. J., Cytotoxicity of anthrax lethal toxin to human acute myeloid leukemia cells is nonapoptotic and dependent on extracellular signal-regulated kinase 1/2 activity. *Transl. Oncol.* **2013,** *6* (1), 25-32.
50. Bekdash, A.; Darwish, M.; Timsah, Z.; Kassab, E.; Ghanem, H.; Najjar, V.; Ghosn, M.; Nasser, S.; El-Hajj, H.; Bazerbachi, A.; Liu, S.; Leppla, S. H.; Frankel, A. E.; Abi-Habib, R. J., Phospho-MEK1/2 and uPAR Expression Determine Sensitivity of AML Blasts to a Urokinase-Activated Anthrax Lethal Toxin (PrAgU2/LF). *Transl. Oncol.* **2015,** *8* (5), 347-57.
51. Thompson, D. W.; Ito, A.; Meyer, T. J., Ru(bpy)(3) (2+)* and other remarkable metal-to-ligand charge transfer (MLCT) excited states. *Pure Appl. Chem.* **2013,** *85* (7), 1257-1305.
52. Mauro, M.; De Paoli, G.; Otter, M.; Donghi, D.; D'Alfonso, G.; De Cola, L., Aggregation induced colour change for phosphorescent iridium(iii) complex-based anionic surfactants. *Dalton Trans.* **2011,** *40* (45), 12106-12116.
53. McGoorty, M. M.; Khnayzer, R. S.; Castellano, F. N., Enhanced photophysics from self-assembled cyclometalated Ir(iii) complexes in water. *Chem. Commun.* **2016,** *52* (50), 7846-7849.
54. Suzuki, K.; Kobayashi, A.; Kaneko, S.; Takehira, K.; Yoshihara, T.; Ishida, H.; Shiina, Y.; Oishi, S.; Tobita, S., Reevaluation of absolute luminescence quantum yields of standard solutions using a spectrometer with an integrating sphere and a back-thinned CCD detector. *PCCP* **2009,** *11* (42), 9850-9860.
55. Kuimova, M. K.; Collins, H. A.; Balaz, M.; Dahlstedt, E.; Levitt, J. A.; Sergent, N.; Suhling, K.; Drobizhev, M.; Makarov, N. S.; Rebane, A.; Anderson, H. L.; Phillips, D., Photophysical properties and intracellular imaging of water-soluble porphyrin dimers for two-photon excited photodynamic therapy. *Org. Biomol. Chem.* **2009,** *7* (5), 889-96.
56. Wilkinson, F.; Helman, W. P.; Ross, A. B., Rate Constants for the Decay and Reactions of the Lowest Electronically Excited Singlet State of Molecular Oxygen in Solution. An Expanded and Revised Compilation. *J. Phys. Chem. Ref. Data* **1995,** *24* (2), 663-677.
57. Abdel-Shafi, A. A.; Beer, P. D.; Mortimer, R. J.; Wilkinson, F., Photosensitized Generation of Singlet Oxygen from (Substituted Bipyridine)ruthenium(II) Complexes. *Helv. Chim. Acta* **2001,** *84* (9), 2784-2795.
58. Garcìa-Fresnadillo, D.; Georgiadou, Y.; Orellana, G.; Braun, A. M.; Oliveros, E., Singlet-Oxygen (1Δg) Production by Ruthenium(II) complexes containing polyazaheterocyclic ligands in methanol and in water. *Helv. Chim. Acta* **1996,** *79* (4), 1222-1238.
59. Ogilby, P. R.; Foote, C. S., Chemistry of singlet oxygen. 42. Effect of solvent, solvent isotopic substitution, and temperature on the lifetime of singlet molecular oxygen. *J. Am. Chem. Soc.* **1983,** *105* (11), 3423-3430.
60. Arnaoutakis, G.; Gakamsky, A.; Nather, D.; Fenske, R. *Detection of Singlet Oxygen*; Edinburgh Instruments Ltd.: 2015; pp 1-8.
61. Caspar, J. V.; Meyer, T. J., Photochemistry of tris(2,2'-bipyridine)ruthenium(2+) ion (Ru(bpy)32+). Solvent effects. *J. Am. Chem. Soc.* **1983,** *105* (17), 5583-5590.
62. Durham, B.; Caspar, J. V.; Nagle, J. K.; Meyer, T. J., Photochemistry of tris(2,2'-bipyridine)ruthenium(2+) ion. *J. Am. Chem. Soc.* **1982,** *104* (18), 4803-4810.
63. Khnayzer, R. S.; Thoi, V. S.; Nippe, M.; King, A. E.; Jurss, J. W.; El Roz, K. A.; Long, J. R.; Chang, C. J.; Castellano, F. N., Towards a comprehensive understanding of visible-light photogeneration of hydrogen from water using cobalt(ii) polypyridyl catalysts. *Energy Environ. Sci.* **2014,** *7* (4), 1477-1488.
64. Collin, J.-P.; Jouvenot, D.; Koizumi, M.; Sauvage, J.-P., Light-Driven Expulsion of the Sterically Hindering Ligand L in Tris-diimine Ruthenium(II) Complexes of the Ru(phen)2(L)2+ Family: A Pronounced Ring Effect. *Inorg. Chem.* **2005,** *44* (13), 4693-4698.
65. Kalyanasundaram, K., Photophysics, photochemistry and solar energy conversion with tris(bipyridyl)ruthenium(II) and its analogues. *Coord. Chem. Rev.* **1982,** *46* (0), 159-244.
66. Azar, D. F.; Audi, H.; Farhat, S.; El-Sibai, M.; Abi-Habib, R. J.; Khnayzer, R. S., Phototoxicity of strained Ru(ii) complexes: is it the metal complex or the dissociating ligand? *Dalton Trans.* **2017,** *46* (35), 11529-11532.
67. Albani, B. A.; Peña, B.; Leed, N. A.; de Paula, N. A. B. G.; Pavani, C.; Baptista, M. S.; Dunbar, K. R.; Turro, C., Marked Improvement in Photoinduced Cell Death by a New Tris-heteroleptic Complex with Dual Action: Singlet Oxygen Sensitization and Ligand Dissociation. *J. Am. Chem. Soc.* **2014,** *136* (49), 17095-17101.
68. Pavani, C.; Iamamoto, Y.; Baptista, M. S., Mechanism and Efficiency of Cell Death of Type II Photosensitizers: Effect of Zinc Chelation. *Photochem. Photobiol.* **2012,** *88* (4), 774-781.

69. Pavani, C.; Uchoa, A. F.; Oliveira, C. S.; Iamamoto, Y.; Baptista, M. S., Effect of zinc insertion and hydrophobicity on the membrane interactions and PDT activity of porphyrin photosensitizers. *Photochem. Photobiol. Sci.* **2009,** *8* (2), 233-240.
70. Snyder, J. W.; Lambert, J. D. C.; Ogilby, P. R., 5,10,15,20-Tetrakis(N-Methyl-4-Pyridyl)-21 H,23H-Porphine (TMPyP) as a Sensitizer for Singlet Oxygen Imaging in Cells: Characterizing the Irradiation-dependent Behavior of TMPyP in a Single Cell. *Photochem. Photobiol.* **2006,** *82* (1), 177-184.

ASSOCIATED CONTENT

Appendix A. Supporting Information

Single wavelength kinetic decay of TA traces, emission lifetime measurements in aerated and dearated water, absorption spectra as a function of irradiation, H^1 NMR, HPLC data, flow cytometry, cell cycle analysis, and analysis of cell cytotoxicity.

AUTHOR INFORMATION

Corresponding Author

* rony.khnayzer@lau.edu.lb

Author Contributions

All authors have given approval to the final version of the manuscript. ‡H.A. and D.A. contributed equally to this work.

Notes

The authors declare no competing financial interests.